RSC Advances

ROYAL SOCIETY OF CHEMISTRY

www.rsc.org/advances

Synthesis, characterization and adsorption properties of amide-modified hyper-cross-linked resin

Jianhan Huang*, Xiaomei Wang, Prafulla D Patil, Jin Tang, Limiao Chen, You-Nian Liu

College of Chemistry and Chemical Engineering, Central South University, Changsha, Hunan 410083, China

* Corresponding author. E-mail address: jianhanhuang@csu.edu.cn (Jianhan Huang).

Abstract

Friedel-Crafts reaction, amination reaction and acetylation reaction were performed to chloromethylated polystyrene (CMPS), and amide-modified hyper-cross-linked resin, HCP-EDA-AA, was prepared. The prepared HCP-EDA-AA owned predominant nanopores and medium polarity, making it possess superior adsorption performance to salicylic acid as compared with the raw material CMPS and the intermediate products, hyper-cross-linked polymer (HCP) and the ethylenediamine-modified hyper-cross-linked resin (HCP-EDA). The Langmuir model characterized the equilibrium data better than the Freundlich model. At a feed concentration of 800.5 mg/L and a flow rate of 67 ml/h, the dynamic capacity of salicylic acid on HCP-EDA-AA was 267.8 mg/g, very close to the extrapolated value by the Langmuir model (273.9 mg/g). The HCP-EDA-AA resin column adsorbed by salicylic acid was almost regenerated by a mixed desorption solvent including 0.01 mol/L of sodium hydroxide (w/v) and 20% of ethanol (v/v). HCP-EDA-AA was repeatedly used for nine times and the equilibrium capacity for the nine time reached 95.5% of the equilibrium capacity for the first time.

Keywords: Hyper-cross-linked resin, adsorption, equilibrium, breakthrough, salicylic acid

1. Introduction

In 1969, Davankov et al proposed a fundamentally novel approach for preparation of the uniformly cross-linked polystyrene [1], and the basic principle of this approach is formulated as intensive cross-linking of polymeric chains by forming rigid cross-linking bridges between two phenyl rings, which leads to creation of a novel type of polymeric materials with special structure and peculiar properties. This type of polymeric materials is termed as hyper-cross-linked polymer (HCP).

HCP is generally synthesized from linear polystyrene or low cross-linked polystyrene with bi-functional cross-linking reagents in the presence of Friedel-Crafts catalysts [2]. Bis-chloromethyl derivatives such as *p*-xylylene dichloride (XDC), 1,4-bis-(chloromethyl)-diphenyl (CMDP) and 1,3,5-tris-(chloromethyl)mesitylene (CMM) are found the preferable bi-functional cross-linking reagents [3, 4], and anhydrous aluminum chloride, iron (III) chloride, zinc chloride and stannic (IV) chloride are shown the excellent Friedel-Crafts catalysts. Monochlorodimethyl ether (MCDE) can react with low cross-linked polystyrene quantitatively through a typical chloromethylation, and the introduced chloromethyl groups on the polystyrene can further react with another phenyl ring under the help of Friedel-Crafts catalysts at a higher temperature, resulting in the further cross-linking of the polystyrene and formation of HCP [5, 6]. The obtained HCP consists of an intensive bridging of strongly solvated polystyrene chains with conformationally rigid cross-linking, and the pore diameter distribution transfers from predominant mesopores to nanopores [7], and hence resulting in a great increase of the Brunauer-Emmet-Teller (BET) surface area and pore volume [8, 9]. Because of these significant changes, HCP is proven efficient polymeric adsorbent for adsorptive removal of non-polar and weakly polar aromatic compounds from aqueous solution [10].

HCP is highly hydrophobic, and it is inconvenient in practical application because a

tedious process is required so that it can be applied in aqueous solution. Moreover, HCP possesses a relatively lower equilibrium capacity to polar aromatic compounds. In order to increase its equilibrium capacity to polar aromatic compounds, HCP is often chemically modified by introduction of polar units into the copolymers, using polar compounds as the cross-linking reagent and addition of polar compounds in the Friedel-Crafts reaction [11, 12]. Amide groups are shown efficient functional groups for improving the equilibrium capacity due to formation of possible hydrogen bond between the amide groups and the adsorbate [13-16]. If amide groups can be uploaded on the surface of HCP, in addition to the excellent pore structure of HCP, the polarity matching between the chemically modified HCP and the adsorbate will also have an advantageous effect on the adsorption. Hence, three typical chemical reactions (Friedel-Crafts reaction, amination reaction and acetylation reaction) were performed for the chloromethylated polystyrene (CMPS) to obtain a novel HCP functionalized by amide groups, and the adsorption behaviors of the obtained HCP was evaluated using salicylic acid as the adsorbate, the adsorption equilibrium and breakthrough dynamics were measured and analyzed in detail.

2. Experimental section

2.1 Materials

CMPS was purchased from Langfang Chemical Co. Ltd., China. The cross-linking degree of CMPS was 6% and the chlorine content was 17.3%. BET surface area, Langmuir surface area and the average pore diameter of CMPS was 28.02 m^2/g, 46.86 m^2/g and 25.2 nm, respectively. Ethylenediamine, acetic anhydride and salicylic acid (C_6H_4(*o*-OH)COOH, Molecular weight: 138.1) were analytical reagents and used without further purification.

2.2 Synthesis of the amide-modified hyper-cross-linked resin

As shown in Scheme S1, the amide-modified hyper-cross-linked resin, HCP-EDA-AA, was prepared from CMPS by three consecutive chemical reactions named Friedel-Crafts reaction, amination reaction and acetylation reaction. The Friedel-Crafts reaction of CMPS was performed following an established procedure [17] and the HCP was produced in this reaction. The method in ref [18] was employed for amination of the HCP. 20 g of HCP was immersed in 60 ml of ethylenediamine for 12 h, the reaction mixture was then kept at 323 K for 15 h, and the ethylenediamine-modified hyper-cross-linked resin, HCP-EDA, was synthesized accordingly. For the acetylation reaction, HCP-EDA was firstly swollen by 80 ml of benzene for 12 h, and then 25 ml of acetic anhydride was added into the reaction mixture. The reaction mixture was refluxed for 10 h and hence the amide-modified hyper-cross-linked resin, HCP-EDA-AA, was prepared.

For the raw material CMPS, the intermediate products HCP, HCP-EDA, and the final product HCP-EDA-AA, a typical purification method was employed to remove the residual impurities in their pores. The solid particles were successively rinsed by 1% of hydrochloric acid aqueous solution (w/v), de-ionized water, 1% of sodium hydroxide aqueous solution (w/v) and de-ionized water until neutral pH. After that, they were extracted by anhydrous ethanol for 10 h and dried under vacuum at 323 K for 10 h.

2.3 Characterization of the resins

The chorine content of the resin was measured by the Volhard method [17] and the weak basic exchange capacity of the resin was determined by another established method in ref [18]. The BET specific surface area, pore volume and pore diameter distribution of the resin were determined from N_2 adsorption-desorption isotherms at 77 K using a Micromeritics Tristar 3000 surface area and porosity analyzer. The Fourier transform infrared spectroscopy (FT-IR) of the resin was collected by KBr disks on a Nicolet 510P Fourier transform infrared instrument.

2.4 Equilibrium adsorption

About 0.1 g of the resin was accurately weighed and mixed with a series of 50 ml of salicylic acid solutions. The initial concentration of salicylic acid solutions was pre-set to be 201.6, 403.2, 604.8, 806.4 and 1008 mg/L, respectively. The series of mixed solutions were shaken at an agitation speed of 180 rpm and a desired temperature (298, 308 or 318 K, respectively) until adsorption equilibrium was reached after eight hours. The absorbency of a standard salicylic acid solution with different known concentrations was analyzed by a UV-2450 spectrophotometer at the wavelength of 296.5 nm. A well-fitted working curve was obtained for salicylic acid, and the absorbency of the salicylic acid solution adsorbed by the resin was measured and the equilibrium concentration of salicylic acid was calculated based on the working curve. The accurate equilibrium capacity of salicylic acid on the resin was calculated based on the following equation:

$$q_e = (C_0 - C_e)V / W \qquad (Eq.1)$$

where q_e was the equilibrium capacity of salicylic acid on the resin (mg/g), C_0 and C_e were the initial and the equilibrium concentration (mg/L) of salicylic acid, , respectively. V was the volume of the salicylic acid solution (L) and W was the mass of the resin (g).

2.5 Dynamic adsorption and desorption

3.01 g of resin was accurately weighed and immersed in de-ionized water for 24 h. These wetted resins were then packed in a glass column densely to assembly a resin column (the volume of the wetted resin was 8 ml, 1BV). The initial salicylic acid solution at a feed concentration of 800.5 mg/L was passed through the resin column at a flow rate of 8.4 BV/h and the concentration of salicylic acid in the effluent from the column exit, C (mg/L), was continuously recorded until it reached the feed concentration. After the adsorption breakthrough run, the resin column was rinsed by 10 ml of de-ionized water and 0.01 mol/L of sodium hydroxide (w/v) and 20% of ethanol (v/v) were applied for regeneration of the resin colum. 30 BV of the desorption solvent was passed through the resin column at a flow rate of 4.2 BV/h and the concentration of salicylic acid was determined until it was zero.

3. Results and discussion

3.1 Characters of the resins

After the Friedel-Crafts reaction, the residual chlorine content of the resin sharply decreased from 17.3% to 4.62% (Table 1), the C-Cl stretching of chloromethyl groups at 1263 cm^{-1} in the FT-IR was significantly weakened (Fig. 1) [19] and the peak in relation to the chlorine atom in the EDS was greatly decreased (Fig. 2), demonstrating that most of the chlorine of CMPS were consumed. After amination reaction of HCP with ethylenediamine, the chlorine content of the resin further decreased to 1.02%, while 1.045 mmol/g of weak basic exchange capacity was measured for HCP-EDA. The C-Cl stretching was further weakened, while the C-N stretching at 1109 cm^{-1}, N-H deformation at 1501 cm^{-1} and N-H stretching at 3400 cm^{-1} appeared in the FT-IR [20]. Furthermore, the peak related to the nitrogen of HCP-EDA presented in the EDS. These results indicated that the amino groups substituted the residual chlorine and were uploaded on the surface of the HCP. After the acetylation reaction of HCP-EDA with acetic anhydride, the weak basic exchange capacity decreased from 1.045 to 0.225 mmol/g, the N-H stretching was much weakened, while strong C=O stretching of amide at 1650 cm^{-1} emerged in the FT-IR, implying that the amino groups were acetylated and the amide-modified hyper-cross-linked resin, HCP-EDA-AA, was prepared.

The BET surface area and pore volume of HCP rapidly increased from 28.02 m^2/g and 0.0033 cm^3/g to 901.3 m^2/g and 0.5820 cm^3/g, respectively (Table 1), the N_2 adsorption amount on HCP was much larger than CMPS at the same relative pressure (P/P^0) (Fig. 3), suggesting that abundant methylene cross-linking bridges were formed after the Friedel-Crafts reaction [21]. This big change induced predominant nanopores for the HCP, and 493.8 m^2/g of t-plot micrpore surface area and 0.2701 cm^3/g t-plot micrpore volume were measured. Additionally, the main pore diameter distribution was transformed to the nanopores (Fig. 4),

and the average pore diameter decreased from 25.2 nm to 2.77 nm, the surface was much smoother after the reaction (Fig. 5). After the amination and acetylation of the HCP, the BET surface area and pore volume were slightly decreased, which might be from the increased polarity due to uploading of the polar amino groups and the amide groups on the surface, and the surface of the resin is rougher with many fissures [22].

Another amide-modified hyper-cross-linked resin HJ-Z01 was prepared in Ref. [16], the difference between this work and Ref [16] is that we replaced the monoamine (methylamine) with a diamine (ethylenediamine) for the amination of the HCP. It is clear that this small change has a great influence on the characteristics of the two resins. First, the weak basic exchange capacity of HJ-Z01 and HCP-EDA-AA is quite different, which indicative of their different chemical structure and polarity. 0.225 mmol/g of amino groups and 0.82 mmol/g of amide groups are uploaded on HCP-EDA-AA, which are much higher than those of HJ-Z01 (0.18 mmol/g of amino groups and 0.64 mmol/g of amide groups). That is, the polarity of HCP-EDA-AA is much greater than that of HJ-Z01. Uploading 1 mol of ethylenediamine on the resin will increase 2 mol of weak basic exchange capacity for the obtained resin, while only 1 mol of weak basic exchange capacity is obtained as 1 mol of methylamine is uploaded on the resin. Hence, diamine is more preferable for increasing the polarity of the resin as the amination reagent [23]. Secondly, the pore structure of these two resins is quite different. The BET surface area and pore volume (especially the t-plot micropore surface area and t-plot micropore volume) of HJ-Z01 is quite higher than those of HCP-EDA-AA.

3.2 Comparison of adsorption of salicylic acid on HCP, HCP-EDA and HCP-EDA-AA

The BET surface area and pore volume of HCP-EDA-AA are much less than those of HJ-Z01, and we propose that the phenol adsorption on HCP-EDA-AA should be much lower than HJ-Z01, In fact, the adsorption isotherm of phenol on HCP-EDA-AA is much weakened

in comparison with HJ-Z01 (Fig. S1). In addition, the phenol adsorption of HCP-EDA-AA is weakened in comparison with the HCP and HCP-EDA due to the much decreased BET surface area and pore volume. However, the polarity of HCP-EDA-AA is much higher than that of HJ-Z01, the polarity matching (the uploading amino groups and amide groups on HCP-EDA-AA can interact with the functional groups of the polar compounds like salicylic acid) will enhance the adsorption of the polar compounds on the resin [22, 23]. Hence, we select salicylic acid as the adsorbate for the adsorption comparison in the present study. Fig. 6 shows the adsorption isotherms of salicylic acid on HCP, HCP-EDA and HCP-EDA-AA at 298 K. The equilibrium capacity of salicylic acid on HCP-EDA-AA is shown the largest among the three resins, and the equilibrium capacity of salicylic acid on HCP-EDA is a bit larger than HCP, which suggests that chemical modification of HCP by uploading the amino and amide groups is necessary. At an equilibrium concentration of 100 mg/L, the equilibrium capacity of salicylic acid on HCP, HCP-EDA and HCP-EDA-AA is predicted to be 118.9, 159.2 and 202.4 mg/g, respectively.

As compared the equilibrium capacity of salicylic acid on HCP-EDA-AA with some other adsorbents, it is found that HCP-EDA-AA are much superior to the polystyrene-type XAD-4 [23], polyacrylate-type XAD-7 [23] as well as the low-cost materials such as Bentonite and kaolin [24]. As compared the equilibrium capacity of salicylic acid on HCP-EDA-AA with those reported in our previous work, it can be concluded that the equilibrium capacity of salicylic acid on HCP-EDA-AA is larger than HJ-L02 (bisphenol-A-modified hyper-cross-linked resin) [25], HJ-Y15 (a hydroquinone-modified hyper-cross-linked resin) [26], HJ-G02 (a β-naphthol-modified hyper-cross-linked resin) [27] and HJ-W02 (a acetanilide-modified hyper-cross-linked resin) [28]. In addition, the equilibrium capacity of salicylic acid on HCP-EDA-AA is comparable with that on HJ-M01 (a diethylenetriamine-modified resins) [23].

Langmuir and Freundlich models are the two typical models for description of the adsorption [29, 30]. The Langmuir model is the best-known model for description of the equilibrium adsorption. It assumes that the adsorption occurs on a structurally homogeneous adsorbent, and all the adsorption sites are energetically identical [29]. The Langmuir model can be expressed as:

$$q_e = \frac{K_L C_e q_m}{1 + K_L C_e} \qquad (Eq.2)$$

where q_m is the maximum capacity (mg/g) of the adsorbate on the adsorbent and K_L is the Langmuir constant related to the adsorption affinity (L/g). It can be linearized as:

$$C_e/q_e = C_e/q_m + 1/(q_m \cdot K_L) \qquad (Eq.3)$$

The Freundlich model is the earliest known model that describes the surface heterogeneity of the adsorbent [30]. It considers multilayer adsorption process with a heterogeneous energetic distribution of the active adsorption sites, and which are accompanied by interactions between adsorbed adsorbates. The Freundlich model can be arranged as:

$$q_e = K_F C_e^{1/n} \qquad (Eq.4)$$

where K_F ([(mg/g)(L/mg)$^{1/n}$]) and n are the characteristic Freundlich constants. The linear Freundlich model can be displayed as:

$$\log q_e = \frac{1}{n} \log C_e + \log K_F \qquad (Eq.5)$$

The linear Langmuir and Freundlich models were used to fit the isotherm data and the corresponding parameters q_m, K_L, K_F and n, as well as the correlation coefficients R^2 and the errors are summarized in Tables 2. It is obvious that the Langmuir model is more suitable for correlating the equilibrium isotherm data. q_m of salicylic acid on HCP-EDA-AA is the largest among the three resins and q_m on HCP-EDA is a bit larger than HCP. In particular, K_L of HCP-EDA-AA is the greatest among the three resins, implying that the adsorption affinity of salicylic acid on HCP-EDA-AA is the strongest.

3.3 Equilibrium adsorption

Fig. 7 plots the equilibrium isotherms of salicylic acid adsorption on HCP-EDA-AA with the temperature at 298, 308 and 318 K, respectively. It is clear that the equilibrium capacity increases with increasing of the equilibrium concentration while decreases with increment of the temperature, implying that the adsorption is an exothermic process [31]. Table 3 summarizes the corresponding parameters by fitting the equilibrium date according to the Langmuir and Freundlich models. It is found that the isotherm data can be well fitted by Langmuir model (R^2>0.99) rather than the Freundlich model. At the temperature of 298, 308 and 318 K, q_m are predicted to be 289.9, 257.1 and 243.3 mg/g, and K_L are scaled to be 22.89, 21.17 and 20.25 L/g, respectively, indicating that the adsorption at a higher temperature is less favorable.

3.4 Dynamic adsorption and desorption

Adsorption column performance is a direct measure of an adsorbent's efficacy for wastewater treatment under application conditions [32]. Fig. 9 (a) displays the adsorption breakthrough profile for the adsorption of salicylic acid on HCP-EDA-AA resin column, the initial concentration of salicylic acid was set to be 800.5 mg/L and the flow rate was 8.4 BV/h. HCP, HCP-EDA, XAD-4 and XAD-7 were also used in this study for the comparison. As can be seen in Fig. 9 (a), the breakthrough point (C/C_0=0.05) of salicylic acid on HCP-EDA-AA resin column was 98.2 BV, higher than HCP and HCP-EDA (65.5 and 79.6 BV, respectively), and much higher than the commercial XAD-4 and XAD-7 (20.63 and 42.8 BV, respectively), confirming that HCP-EDA-AA is the most efficient resin for adsorptive removal of salicylic acid among these five resins. The dynamic capacity of salicylic acid on HCP-EDA-AA can be estimated to be 806 mg. By considering the mass of the resin column (3.01 g), and the dynamic equilibrium capacity can be determined to be 267.8 mg/g, very close to the extrapolated value by the Langmuir model (273.9 mg/g).

After the adsorption breakthrough run, different solvents are employed for regeneration of the HCP-EDA-AA resin column, and the recovery efficiency is displayed in Fig. 10. It is evident that water can partly desorb salicylic acid from the resin column, and 23.0% of salicylic acid is desorbed from the resin column. Sodium hydroxide is an effective solvent for regeneration of the HCP-EDA-AA resin column and 88.6% of salicylic acid is desorbed from the resin column as 0.01 mol/L of sodium hydroxide (w/v) is employed as the desorption solvent. In particular, addition of ethanol in the solution of 0.01 mol/L of sodium hydroxide (w/v) can further improve the recovery efficiency, and 99.6% of salicylic acid can be recovered as increasing the concentration of ethanol to 20% (v/v) in 0.01 mol/L of sodium hydroxide (w/v). Hence, a mixed solution including 0.01 mol/L of sodium hydroxide (w/v) and 20% of ethanol (v/v) is applied as the desorption solvent in the dynamic desorption. At a flow rate of 4.2 BV/h, only 15.0 BV of the desorption solvent is enough for regeneration of the resin column, and the dynamic desorption capacity is calculated to be 773.6 mg (Fig. 9 (b)), very close to the dynamic capacity (806.0 mg). HCP-EDA-AA are repeatedly used for nine cycles of continuous adsorption-desorption process, the equilibrium capacity for the nine time reaches 95.5% of the initial equilibrium capacity (Fig. 11), and the adsorbed salicylic acid can be almost desorbed every time. HCP-EDA-AA exhibits good reusability with remarkable regeneration behaviors.

4. Conclusion

HCP-EDA-AA was synthesized from CMPS by three consecutive chemical reactions, and 0.225 mmol/g of amino groups and 0.820 mmol/g of amide groups were uploaded on the surface of HCP-EDA-AA. 379.3 m^2/g of t-plot micropore surface area and 0.2069 cm^3/g of t-plot micropore volume were determined for HCP-EDA-AA, implied that nanopores were predominant for HCP-EDA-AA. The favorable surface polarity and abundant nanopores made HCP-EDA-AA a better adsorption to salicylic acid. The equilibrium data of salicylic acid adsorption on HCP-EDA-AA could be well fitted by Langmuir model. At an initial concentration of 800.5 mg/L and a flow rate of 8.4 BV/h, the dynamic equilibrium capacity was measured to be 267.8 mg/g, and the resin column could be almost desorbed by 0.01 mol/L of sodium hydroxide (w/v) and 20% of ethanol (v/v).

Acknowledgment

We gratefully acknowledged the financial supports by the National Natural Science Foundation of China (No. 21376275, 21174163 and 213111014) and the Shenghua Yuying Project of Central South University.

Notes and references

[1] S.V. Rogozhin, V.A. Davankov, M.P. Tsyurupa, Patent USSR 299165 (1969)

[2] M.P. Tsyurupa, V.A. Davankov, *React. Funct. Polym.* 53 (2002) 193-203.

[3] F. Maya, F. Svec, *Polymer* 55 (2014) 340-346.

[4] M.P. Tsyurupa, V.A. Davankov, *React. Funct. Polym.* 66 (2006) 768-779.

[5] C. Long, P. Liu, Y. Li, A.M. Li, Q.X. Zhang, *Environ. Sci. Technol.* 45 (2011) 4506-4512.

[6] X.M. Wang, K.L. Dai, L.M. Chen, J.H. Huang, Y.N. Liu, *Chem. Eng. J.* 242 (2014) 19-26.

[7] C.G. Oh, J.H. Ahn, S.K. Ihm, *React. Funct. Polym.* 57 (2003) 103-111.

[8] V.A. Davankov, M.P. Tsyurupa, *React. Polym.* 13 (1990) 27-42.

[9] J.H. Ahn, J.E. Jang, C.G. Oh, S.K. Ihm, J. Cortez, D.C. Sherrington, *Macromolecules* 39 (2006) 627-632.

[10] J. Fan, W.B. Yang, A.M. Li, *React. Funct. Polym.* 71 (2011) 994-1000.

[11] C.L. He, J.H. Huang, C. Yan, J.B. Liu, L.B. Deng, K.L. Huang, *J. Hazard. Mater.* 180 (2010) 634-639.

[12] A.M. Li, Q.X. Zhang, G.C. Zhang, J.L. Chen, Z.H. Fei, F.Q. Liu, *Chemosphere* 47 (2002) 981-989.

[13] M.C. Xu, Y. Zhou, J.H. Huang, *J. Colloid Interf. Sci.* 327 (2008) 9-14.

[14] J.H. Huang, Y. Zhou, K.L. Huang, S.Q. Liu, Q. Luo, M.C. Xu, *J. Colloid Interf. Sci.* 316 (2007) 10-18.

[15] J.H. Huang, K.L. Huang, S.Q. Liu, Q. Luo, M.C. Xu, *J. Colloid Interf. Sci.* 315 (2007) 407-414.

[16] J.H. Huang, X.J. Jin, S.G. Deng, *Chem. Eng. J.* 192 (2012) 192-200.

[17] C.P. Wu, C.H. Zhou, F.X. Li, Experiments of Polymeric Chemistry; Anhui Science and Technology Press: Hefei, 1987.

[18] B.L. He, W.Q. Huang, *Ion Exchange and Adsorption Resin*; Shanghai Science and Technology Education Press: Shanghai, 1995.

[19] G.H. Meng, A.M. Li, W.B. Yang, F.Q. Liu, X. Yang, Q.X. Zhang, *Eur. Polym. J.* 43 (2007) 2732-2737.

[20] J.T. Wang, Q.M. Hu, B.S. Zhang,; Y.M. Wang, *Organic Chemistry*; Nankai University Press: Tianjing, 1998.

[21] V.A. Davankov, M.P. Tsyurupa, Hypercrosslinked polymeric networks and adsorbing materials, *Compr. Anal. Chem.* 56 (2011) 1-648.

[22] J.H. Huang, H.W. Zha, X.Y. Jin, S.G. Deng, *Chem. Eng. J.* 195-196 (2012) 40-48.

[23] J.H. Huang, X.Y. Jin, J.L. Mao, B. Yuan, R.J. Deng, S.G. Deng, *J. Hazard. Mater.* 217-218 (2012) 406-415.

[24] F.P. Bonina, M.L. Giannossi, L. Medici, C. Puglia, V. Summa, F. Tateo, *Appl. Clay Sci.* 36 (2007) 77-85.

[25] H.X. Hu, X.M. Wang, S.Y. Li, J.H. Huang, S.G. Deng, *J. Colloid Interf. Sci.* 372 (2012) 108-112.

[26] J.H. Huang, *J. Appl. Polym. Sci.* 121 (2011) 3717-3723.

[27] J.H. Huang**,** G. Wang, K.L. Huang, *Chem. Eng. J.* 168 (2011) 715-721.

[28] J.H. Huang**,** X.L. Wang, X.M. Wang, K.L. Huang, *Ind. Eng. Chem. Res.* 50 (2011) 2891-2897.

[29] I. Langmuir, *J. Am. Chem. Soc.* 38 (1916) 2221-2295.

[30] H.M.F. Freundlich, Z. Phys. Chem. 57A (1906) 385-470.

[31] D.D. Duong, *Adsorption analysis: Equilibria and kinetics*; World Scientific Publishing: Singapore, 1998.

[32] X. Li, K. He, B.C. Pan, S.J. Zhang, L. Lu, W.M. Zhang, *Chem. Eng. J.* 193-194 (2012) 131-138.

Table 1 The characteristic parameters of CMPS, HCP, HCP-EDA and HCP-EDA-AA

	CMPS	HCP	HCP-EDA	HCP-EDA-AA
BET surface area /(m^2/g)	28.02	901.3	807.2	639.4
Langmuir surface area /(m^2/g)	46.86	1336	1194	950.5
t-plot surface area /(m^2/g)	-	493.8	445.0	379.3
Pore volume /(cm^3/g)	0.0033	0.5820	0.5242	0.4222
t-plot pore volume/(cm^3/g)	-	0.2701	0.2429	0.2069
Average pore width /(nm)	25.2	2.77	2.71	2.64
Chlorine content /(%)	17.3	4.62	1.02	-
Weak basic exchange capacity /(mmol/g)	-	-	1.045	0.225

Table 2 The fitted characteristic parameters for the isotherm data of salicylic acid adsorption on HCP, HCP-EDA and HCP-EDA-AA according to linear Langmuir and Freundlich models

	Langmuir model					Freundlich model				
	K_L /(L/g)	Errors	q_m /(mg/g)	Errors	R^2	K_F /([(mg/g)(L/mg)$^{1/n}$])	Errors	n	Errors	R^2
HCP	4.309	0.03324	220.6	1.186×10^{-4}	0.9978	7.283	0.1071	1.684	0.04685	0.9910
HCP-EDA	9.996	0.02062	258.5	7.844×10^{-5}	0.9988	20.23	0.09248	2.324	0.04172	0.9813
HCP-EDA-AA	22.89	0.01020	289.9	4.029×10^{-5}	0.9996	37.07	0.1272	3.745	0.05988	0.9141

Table 3 The fitted parameters for the isotherm data of salicylic acid on HCP-EDA-AA by the Langmuir and Freundlich models

	Langmuir model					Freundlich model				
	K_L /(L/g)	Errors	q_m /(mg/g)	Errors	R^2	K_F /([(mg/g)(L/mg)$^{1/n}$])	Errors	n	Errors	R^2
298 K	22.89	0.01020	289.9	4.029×10^{-5}	0.9996	37.07	0.1272	3.745	0.05988	0.9141
308 K	21.17	0.01204	257.1	4.294×10^{-5}	0.9996	36.63	0.1368	3.229	0.06290	0.8896
318 K	20.25	0.01838	243.3	6.057×10^{-5}	0.9994	33.65	0.1379	3.167	0.06201	0.8962

Fig. 1 FT-IR spectra of CMPS, HCP, HCP-EDA and HCP-EDA-AA

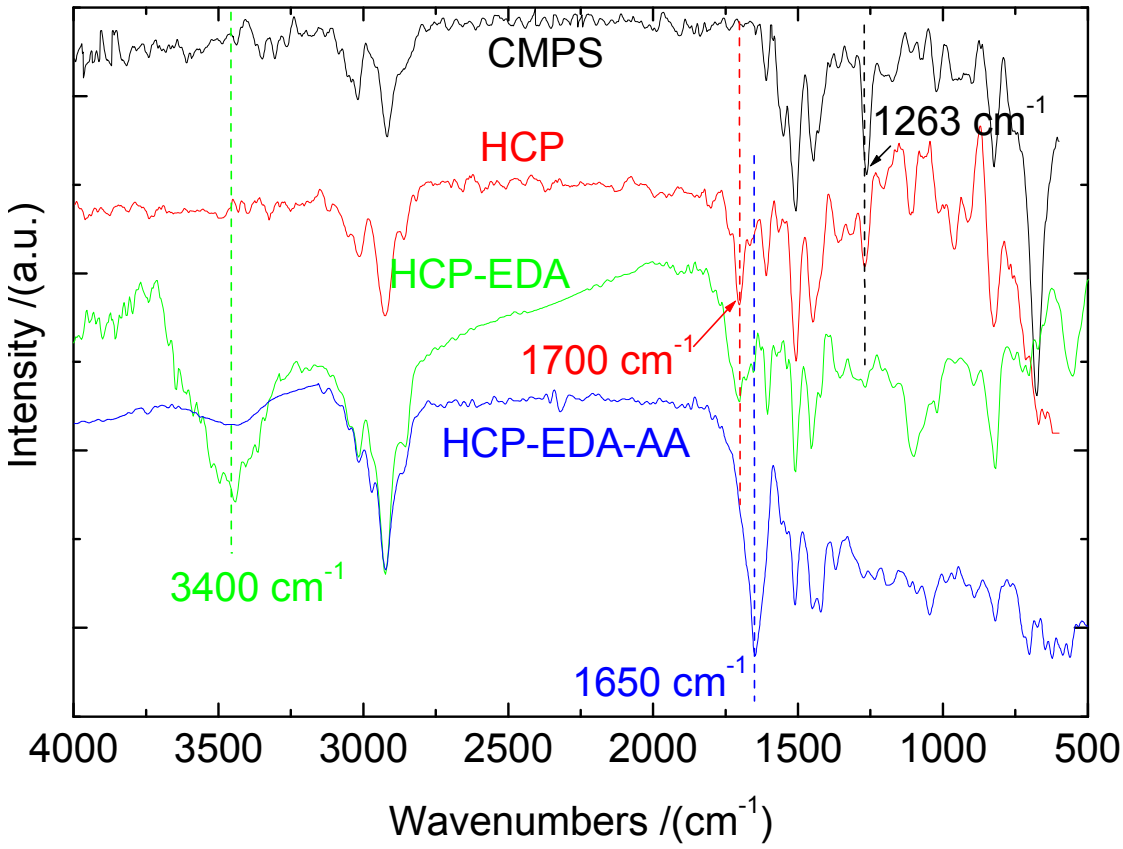

Fig. 2 Energy dispersive X-ray spectroscopy (EDS) of CMPS, HCP, HCP-EDA and HCP-EDA-AA

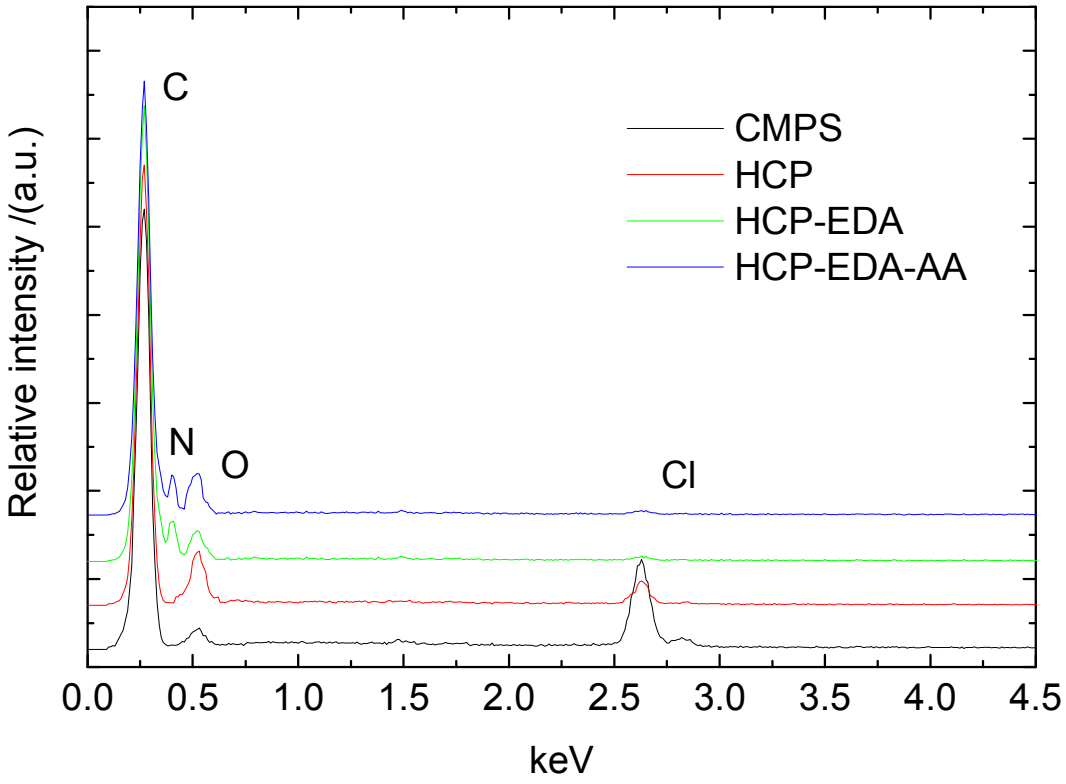

Fig. 3 N_2 adsorption-desorption isotherms of CMPS, HCP, HCP-EDA and HCP-EDA-AA

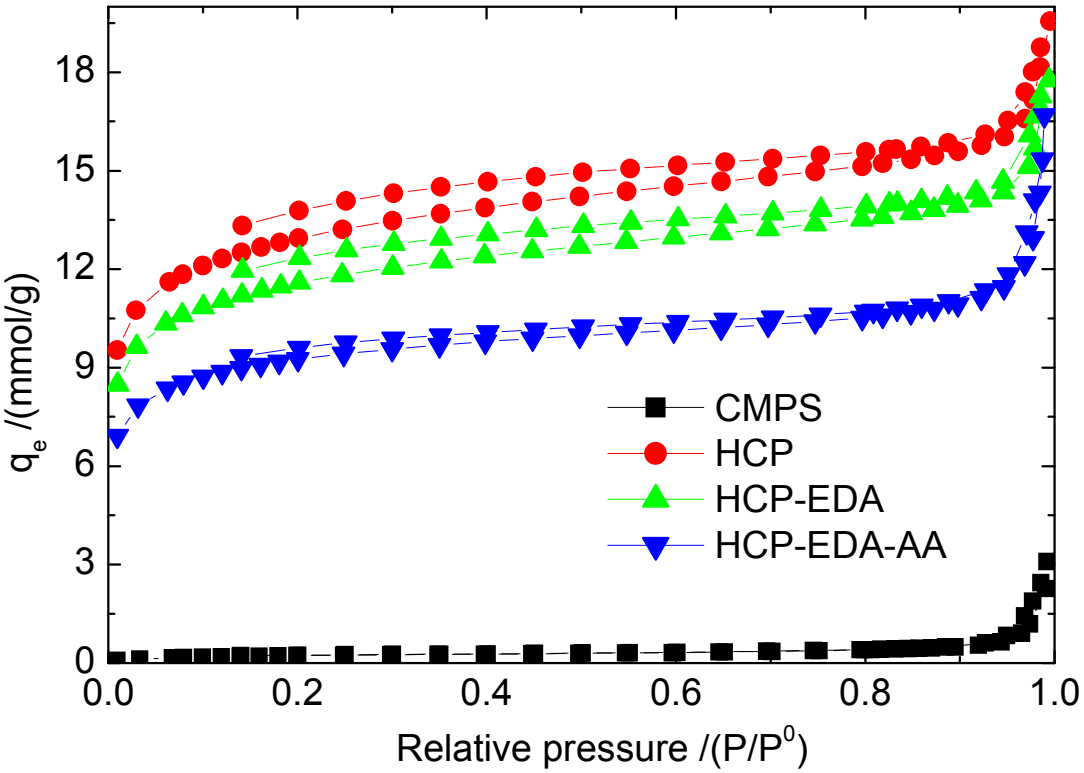

Fig. 4 Pore diameter distribution of CMPS, HCP, HCP-EDA and HCP-EDA-AA

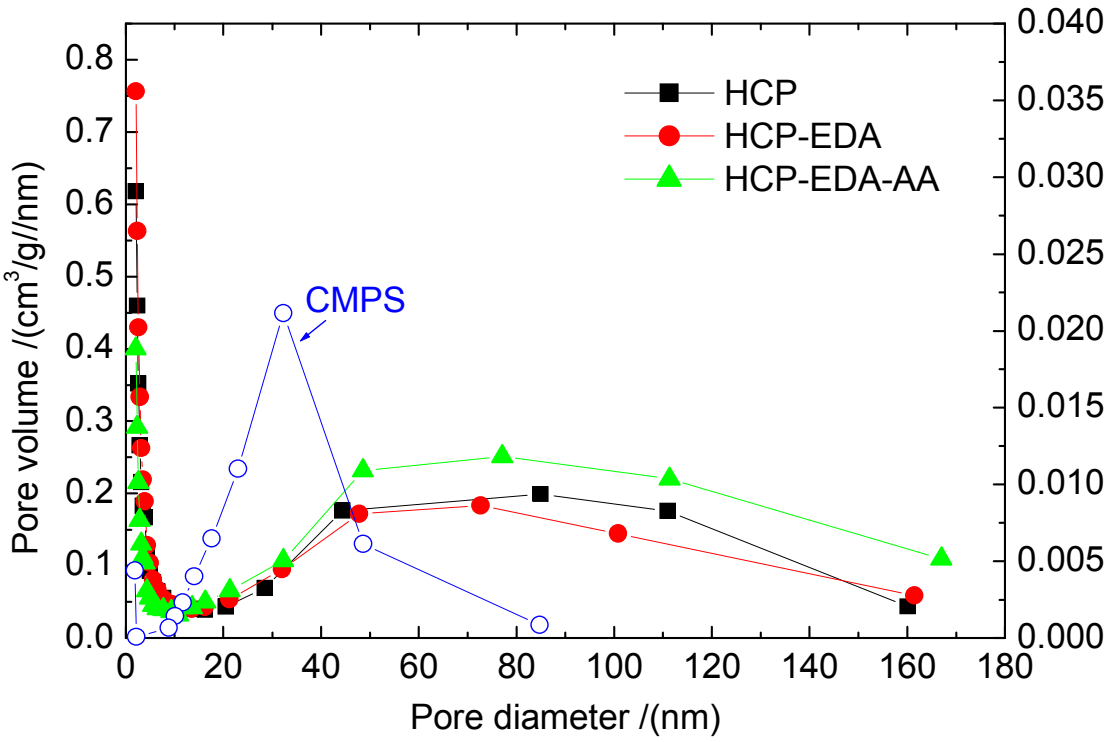

Fig. 5 Scanning electron microscopy (SEM) images of CMPS, HCP, HCP-EDA and HCP-EDA-AA

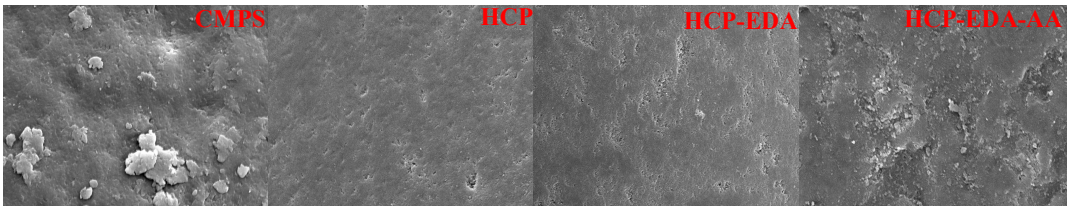

Fig. 6 Comparison of equilibrium capacity of salicylic acid adsorption on HCP, HCP-EDA and HCP-EDA-AA

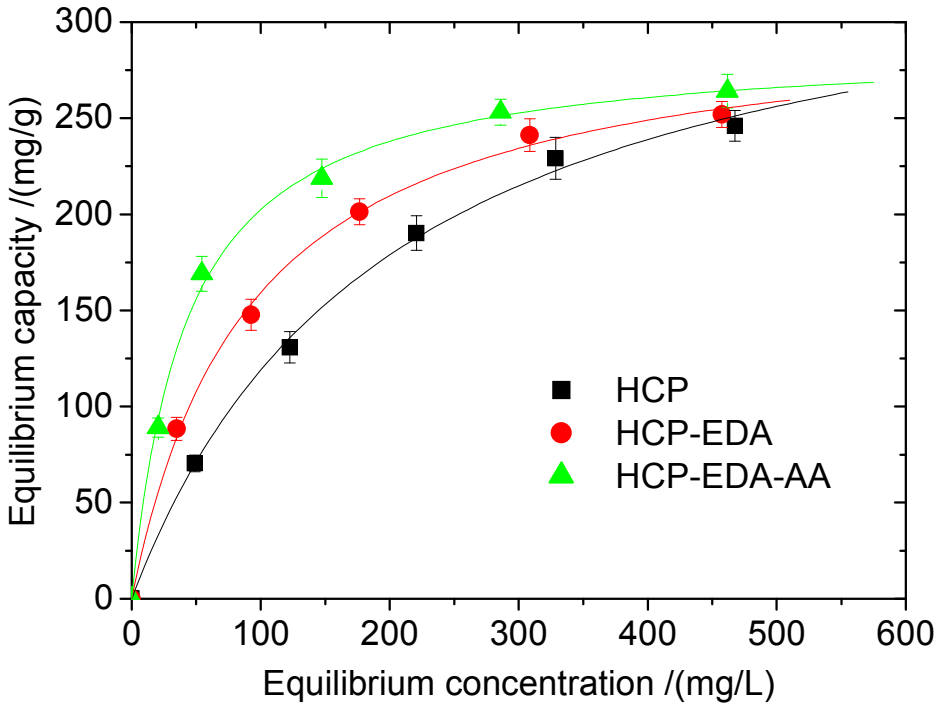

Fig. 7 Adsorption isotherms of salicylic acid on HCP-EDA-AA at 298, 308 and 318 K

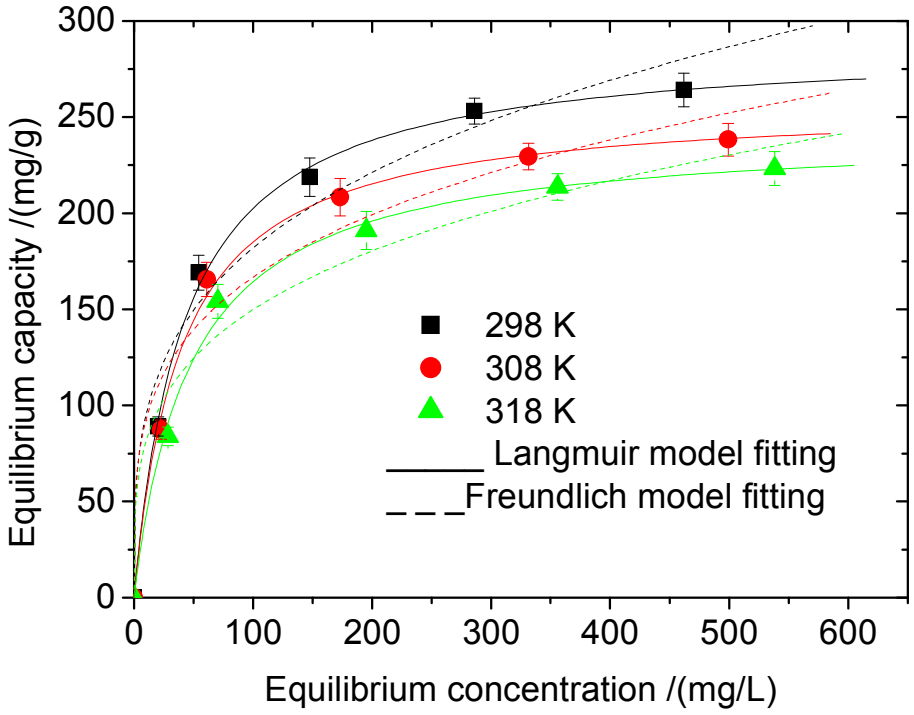

Fig. 8 Plotting of ln K_L with 1/T for adsorption of salicylic acid on HCP-EDA-AA

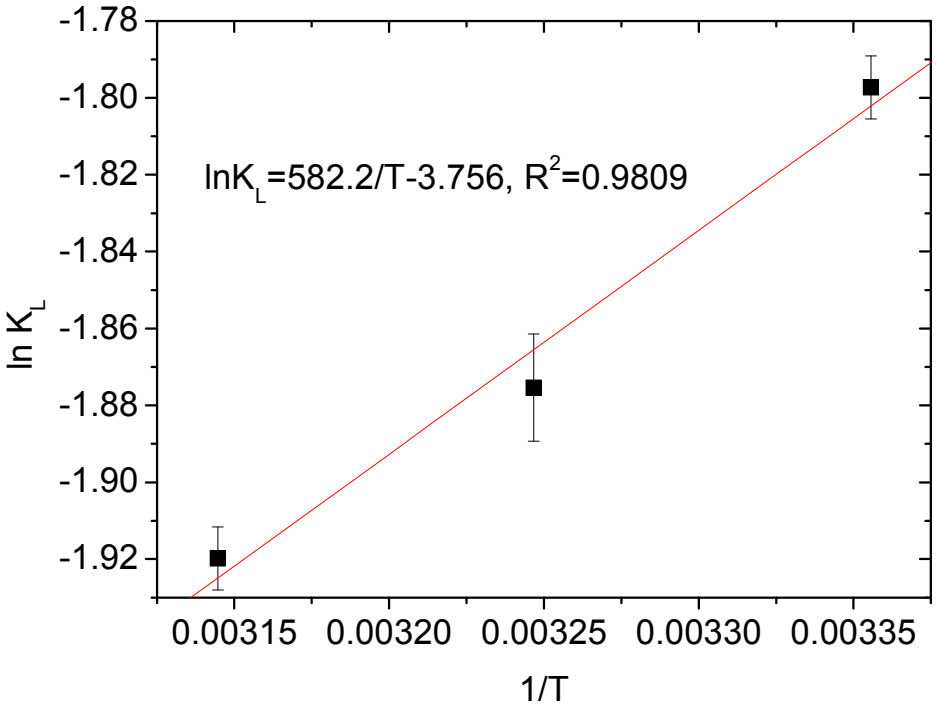

Fig. 9 Dynamic adsorption (a) and desorption (b) curves of salicylic acid on HCP-EDA-AA resin column in comparison with HCP, HCP-EDA, XAD-4 and XAD-7

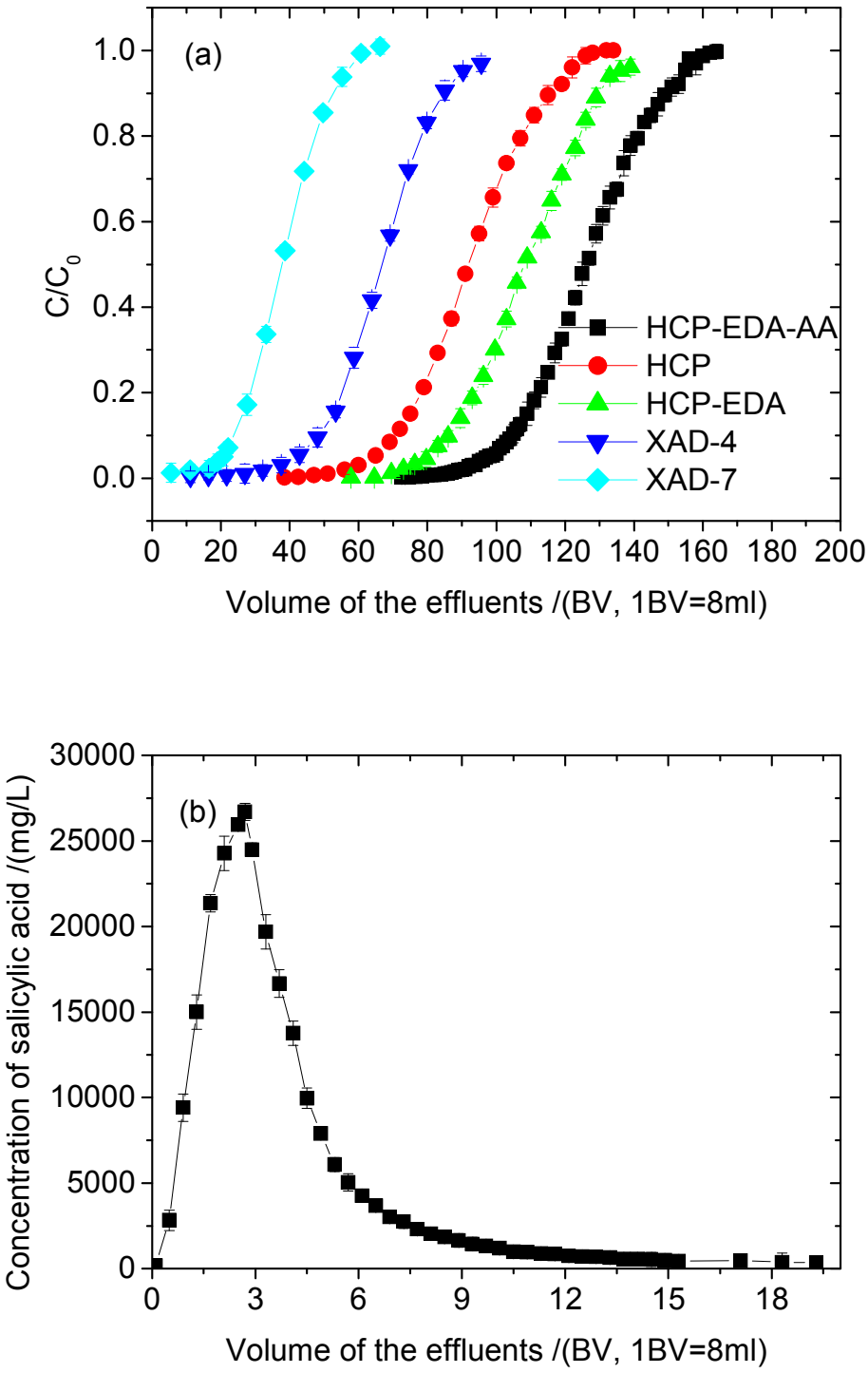

Fig. 10 The recovery efficiency of different solvents for desorption of salicylic acid from HCP-EDA-AA resin column

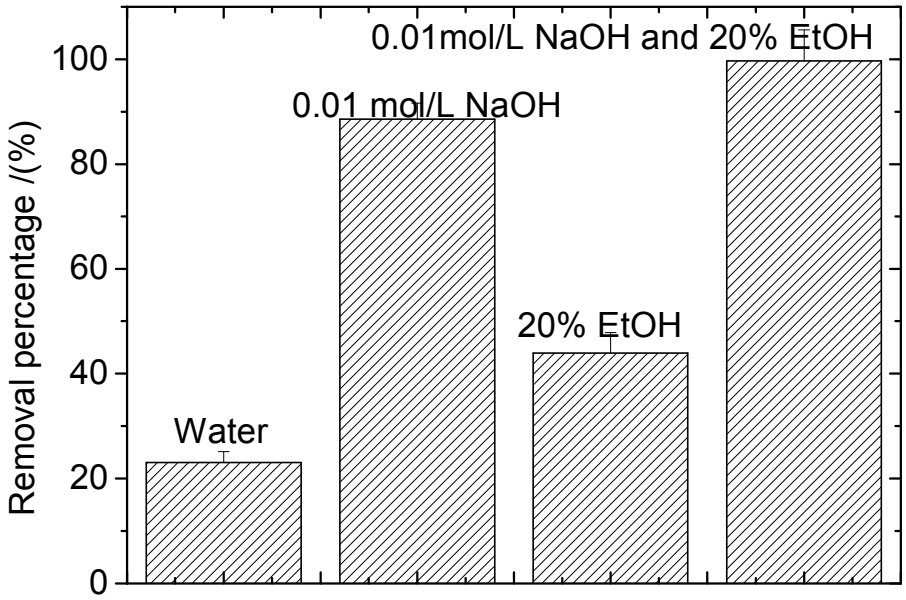

Fig. 11 Effect of recycle number on the equilibrium adsorption/desorption capacity of salicylic acid on HCP-EDA-AA from aqueous solution

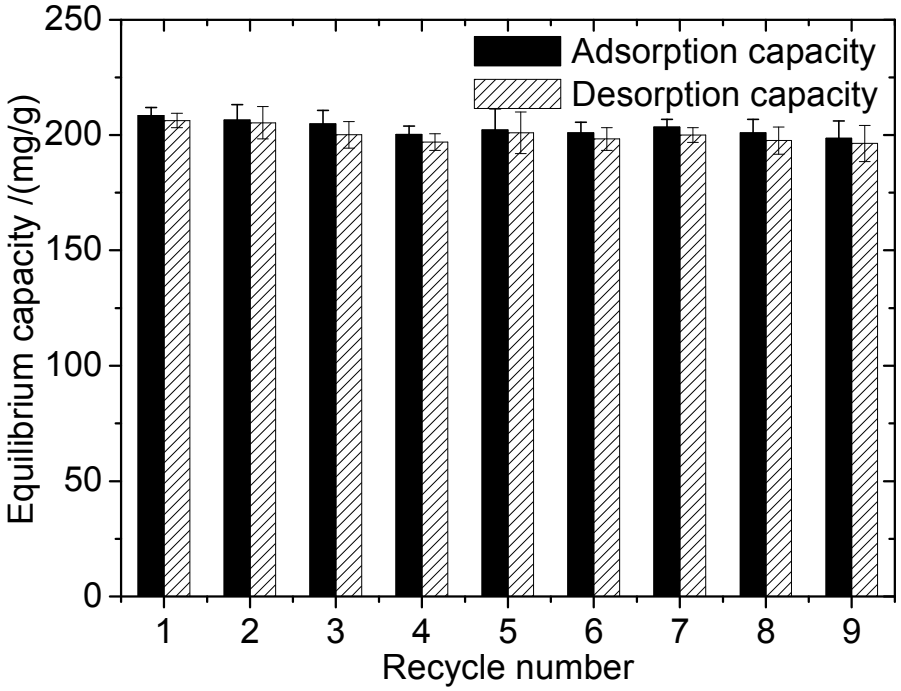

Graphic abstract

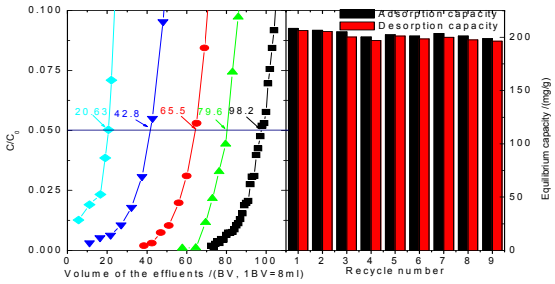

HCP-EDA-AA is an excellent resin for adsorptive removal of salicylic acid and it exhibits good reusability with remarkable regeneration behaviors.